Available online at www.sciencedirect.com
SCIENCE DIRECT®
Surface Science 548 (2004) 187–199
SURFACE SCIENCE
www.elsevier.com/locate/susc

Secondary-electron emission mechanism of LiF film by (e,2e) spectroscopy

S. Samarin [a,*], J. Berakdar [b], A. Suvorova [c], O.M. Artamonov [d], D.K. Waterhouse [a], J. Kirschner [b], J.F. Williams [a]

[a] *Centre for Atomic, Molecular and Surface Physics, Department of Physics, University of Western Australia, 35 Stirling Hwy, Crawley, WA 6009, Australia*
[b] *Max-Planck-Institut für Mikrostrukturphysik, Weinberg 2, D-06120 Halle, Germany*
[c] *Centre for Microscopy and Microanalysis, University of Western Australia, Perth, WA 6009, Australia*
[d] *Research Institute of Physics, St. Petersburg University, St. Petersburg, Russia*

Received 25 August 2003; accepted for publication 4 November 2003

Abstract

Secondary-electron emission (SEE) from LiF films deposited on Si(0 0 1) surface was studied using time-of-flight two-electron coincidence spectroscopy. A set of energy-distribution curves (EDCs) of secondary electrons excited from a LiF film by electrons with energies in the range of 20–50 eV exhibits emission features at about 7 and 11 eV. The energy positions of these maxima do not depend on the incident energy. To reveal the origin of these features, each of the EDCs was spanned in the second dimension E_2 using two-electron coincidence spectroscopy. Two-dimensional mapping of the energy sharing between correlated electrons shows that above 25 eV incident energy, one electron of the pair is preferentially emitted with $E_1 = 7.2 \pm 0.3$ eV energy and the second one with energy $E_2 = (E_p - 23.3) \pm 0.5$ eV, where E_p is the incident electron energy. At about 30 eV incident energy, a second favoured emission energy of 10.9 ± 0.3 eV is observed. The unique capability of (e,2e) spectroscopy established the links between electron energy loss process and emission features in the EDCs.

It is suggested that the mechanism of SEE from LiF film includes the excitation of two collective excitations with subsequent decay via electron ejection. It was shown that the mechanism of secondary emission from LiF film depends on the film thickness and its structure.

Keywords: Alkali halides; Insulating films; Secondary electron emission; Electron–solid interactions, scattering, diffraction

1. Introduction and overview

Upon electron, ion or photon irradiation, the secondary-electron yield from insulators, particularly alkali halides, is typically an order of magnitude higher than from metals. This phenomenon has received much attention due to its potential in the development of sensitive charge-amplification

* Corresponding author. Tel.: +61-9380-3479; fax: +61-9380-1014.
E-mail address: samar@physics.uwa.edu.au (S. Samarin).

0039-6028/$ - see front matter © 2003 Elsevier B.V. All rights reserved.
doi:10.1016/j.susc.2003.11.003

devices such as ion–electron converters and electron multipliers. We present here the results of experimental investigation of the secondary emission mechanism of a LiF film excited by 20–50 eV primary electrons using two-electron coincidence spectroscopy. The paper is organized as follows. An overview of electronic and excitation properties of LiF films and single crystals along with the secondary emission features are presented in this section. A comparison of the two-electron spectroscopy versus electron-energy-loss spectroscopy (EELS) and the unique capability of the (e,2e) technique to establish the relation between the energy loss process and a true secondary emission is also addressed in Section 1. Section 2 describes the experimental details. Experimental results and their discussion are included in Sections 3 and 4, respectively, followed by conclusions.

1.1. Electronic and excitation properties of LiF

An extensive number of experimental and theoretical investigations of the electronic properties of LiF have been carried out [1–33]. The outcome of these studies may be summarized as follows: Experimentally determined band gaps energies (E_g) between the valence and conduction bands are in the range of 13.6 eV [4,5] to 14.2 eV [6]. Corresponding calculations are of two kinds: (a) band calculations or (b) cluster model calculations where a large cluster is embedded in an ionic cage. The band calculation that accounts for electron correlation, gives the band gap as 13.9 eV [24] and 14.0 eV, [25] while the cluster model gives 13.9 eV [28]. The width of the valence band, as determined from photoemission experiments, varies between 3.5 eV [31,32] and 3.7 eV [33]. These numbers are obtained from the full width of half maximum of the angle-integrated valence band photoemission spectra. When using the full width at the peak base a bandwidth as large as 6.1 eV is obtained [33].

Pong and Inouye (quoted in [24]) observed exciton photoemission at 12.6 eV relative to the ground state level, i.e. the top of the valence band, while Gallon [9] observed the exciton at 13.5 eV using EELS. The bulk exciton states (calculated by the band theory and the cluster model with the electron correlation correction) are located at 11.7 eV [24], and 13.4 eV [28] above the ground state, so that the result of the cluster model accords well with the EELS result. The surface exciton has also been observed by EELS [9]; the excitation energy is 3 eV less than that of the bulk exciton, and is predicted accurately by the cluster model. On the other hand recent ab-initio calculations, based on the solution of the Bethe-Salpeter equation for the two-particle Green's function, predicted the occurrence in the optical spectrum of two strongly bound singlet excitons at 12.8 eV (transverse excitons) and a longitudinal singlet exciton at 13.3 eV [29]. The former is confirmed by optical absorption experiments [30] whereas the latter is not visible. A further important quantity as far as the excitation spectrum is concerned is the dynamic structure factors $S(\mathbf{q},\omega)$, which is the Fourier transform in space and time of the time-dependent density–density correlation function. For LiF $S(\mathbf{q},\omega)$ has been measured using inelastic X-ray scattering [34]. The results are in reasonable agreement with those obtained from energy loss spectra [35] in the energy range between 10 and 35 eV. The main observation in the $S(\mathbf{q},\omega)$ spectra is a very narrow exciton peak around 14 eV and a nominal plasmon around 25 eV. (This term is chosen as the calculated real part of the dielectric function crosses zero around 25 eV for momentum transfers of 0.23–0.46ΓX, and it is close to zero for $q = 0.72\Gamma X$ [34–36].) At energies above 35 eV, core hole excitations of F 2s electrons are observed, whereas at 61 eV Li 1s electrons are excited. Further subsidiary peaks are observed, which are related to intermediate transitions. In particular, peaks appearing in the energy range intermediate between the exciton and the plasmon peaks are associated with interband transitions that evolve with momentum transfer. For the lowest momentum transfer, both experiment and theory including electron–hole interaction show peaks at 15 and 18 eV, with the 15 eV one being higher in intensity. Increasing the momentum transfer, the two peaks merge into one peak near 18 eV. Increasing the momentum transfer even further, this peak narrows, indicating that the transitions move closer in energy.

The dependence of the electronic properties of LiF on lattice defects have been demonstrated

theoretically using a cluster embedded model [37]: while calculation [24–26] assuming perfect lattice yielded 14–15 eV as an ionization threshold (I_t) of the fluorine ion band, the calculations that account for lattice defects give the value of surface and bulk ionization thresholds as 8.1 and 8.7 eV, respectively. Refs. [4,5] give the experimental value as 9.8 eV, which is measured as $I_t = E_b(F^-) - 0.5E_{tw}(F^-)$. Here $E_b(F^-)$ is the arithmetic midpoint of the valence fluorine ion band, and $E_{tw}(F^-)$ is the total width of this band ($E_b(F^-) = 12.85$, $E_{tw}(F^-) = 6.1$ eV [4,5]).

1.2. Secondary-electron emission from LiF

Electron emission from insulators, and in particular from alkali halides, following irradiation by electrons, ions or photons is characterized by a high yield and a complicated energy distribution of electrons [38]. An energy-distribution curve (EDC) of electrons, excited from a LiF film by X-ray, exhibits peaks at 7 and 11 eV [39]. These features are observed in the EDCs of secondary-electron emission (SEE) from LiF induced by electrons [40–42]. In cases where secondary electrons are produced by energetic beams (e.g. 1 keV, and higher, incident electron energies or equivalently fast heavy projectiles), one finds basically similar shapes of the secondary electrons spectra regardless of the nature of the incident particle (electron, ion or photon). The physical picture underlying the secondary-electron production is then as follows: The incident particle excites a target electron that can be considered as an internal "primary" projectile electron with energy E_p. If the energy of the electron is high enough it undergoes further collisions and produces individual (electron–hole pairs) or collective excitations (phonons, excitons, plasmons). Each collision leads to a specific energy loss of the primary electron: If the energy E_p of this primary electron is high enough it may suffers from multiple collisions from scattering centers in the sample. When E_p decreases, the energy loss channels are switched off one by one. When E_p descends below the threshold for plasmon excitations, this energy loss channel closes. If E_p is less than the fundamental gap energy E_g then the interband electron–hole pair excitation mechanism is closed. The excitons' thresholds lie below E_g and thus the excitonic channels are the next energy-loss pathway to be closed when E_p further decreases. Phonon excitations requires only few tens of meV at room temperature and therefore this loss mechanism remains open even for very low energy electrons. At any stage of the cascade process the electron can leave the solid surface if its momentum component normal to the surface and its energy is still large enough to escape into the vacuum level. Thus, a smooth secondary emission maximum is formed as a result of the cascade energy loss and the electron multiplication process.

Structures (peaks and dips) in the EDCs of SEE are either due to corresponding structure in the density of unoccupied states, or they can result from the decay of excited individual and collective modes via electron emission. For example, for LiF the aforementioned peak occurring at 7 eV in the EDCs of SEE has been interpreted as the result of plasmon de-excitation via electron emission [39–41]. We recall that in a free-electron-like model of solids, volume plasmons cannot decay in a single electron–hole pair unless their wave vector exceeds a critical value q_c [43]. In a real solid, however, a volume plasmon can decay via interband transitions [44]. Plasmon decay via interband transitions can occur even for plasmons of very long wavelength (almost zero wave vector). In this case, the transition is nearly vertical in the reduced-zone scheme [45]. For a further discussion of the role of plasmon decay in the SEE process one may consult [45,46]. As mentioned above the existence of the bulk plasmon excitations in LiF at $\hbar\omega_p = 25$ eV has been predicted theoretically [47–49] and confirmed by measurements [34,35,50]. The plasmon energy loss at about 25 eV has been observed in electron energy loss spectra (EELS) of LiF films and single crystals [34,51–53]. It should be noted that the shape and width of the plasmon peak is strongly dependent on the amount of the transferred momentum, i.e. it is strongly dispersive.

Due to the plasmon de-excitation via electron emission, a peak in the EDC of secondary electrons appears at the energy E_e. However, the energy and wave vector conservation laws have to be satisfied for this reaction. The energy conservation requires that

$$E_e = \hbar\omega_p - E_g - \Delta E_v - \chi, \quad (1)$$

where E_g is the energy gap, ΔE_v is the half-width of the valence band and χ is the electron affinity. In the case of a single crystal the wave vector conservation law implies that the wave vector of the ejected particles has to be equal to the wave vector of the plasmon.

As mentioned above, for LiF different values of the plasmon energy, the energy gap and the valence bandwidth have been reported. In [54] an affinity of $\chi = -(1.2 \pm 0.2)$ eV has been determined for 17 ML LiF layer using low energy electron transmission spectroscopy. On the other hand, Himpsel and coworkers [55], based on their photoemission data, have estimated the electron affinity to be −2.7 eV. In another publication Himpsel and coworkers [56] provided the value of the affinity as −2.3 eV for a LiF layer grown epitaxially on Ge(1 0 0). The difference in these values stem from different spectroscopic techniques as well as from the different structures of the investigated samples.

The significant differences in the relevant parameters have lead naturally to a controversy in the interpretation of the origin of structures of spectra of the secondary electrons emitted from LiF. For example, the maximum at 6.3 eV in EDC of secondary electrons excited from LiF film by soft X-ray has been identified [39] as the result of a plasmon decay using (1) with the following values of the parameters: $\hbar\omega_p = 25.3$ eV, $E_g = 13.6$ eV, $\Delta E_v = 3.7$ eV, $\chi = 1$ eV. In addition to the 6.3 eV maximum a weak feature at 11 eV was also observed, which was suggested to be related to the maximum of the unoccupied density of states.

In the experiments performed by Gusarov and Murashov [41] a broad maximum at $E_s = 6$ eV has been observed in the EDC of secondary electrons emitted from a single crystal of LiF by primary electrons with energy from 50 to 210 eV. For primary energies above 60 eV an additional structure near 11 eV emerged.

The EDCs of secondary electrons excited by primary electrons with energy 35 eV from LiF film show similar structure with two maxima at 8.3 and 11.9 eV [42]. In this context we mention the observation of SEE from an atomically flat LiF(0 0 1) surface irradiated by fast (0.5 MeV) grazing incidence protons [57]. There was argued that surface plasmons (excited by protons) are converted into electron–hole pairs with a conversion rate close to 100%.

Previous conclusions of studies on the secondary emission spectra of LiF can be roughly summarized as follows: two features are often observed in the energy distribution of secondary electrons: the first—in the energy range between 6 and 8 eV and the second is in the energy range between 10 and 12 eV. They do not depend on the type and energy of the primary particles. Possible explanations of these peaks offered in the literatures are: (1) manifestation of maxima in the density distribution of unoccupied electronic states; (2) plasmon decay via electron emission from the valence band; (3) autoionization process. Our secondary-electron spectra also show the peaks at ~7 and ~11 eV [58]. We will establish the links between energy loss structure and emission feature using two-electron coincidence spectroscopy. For interpretation of these emission maxima we consider the plasmon decay mode. Alternatively we discuss the appearance of these peaks due to the decay of the excitonic states [29,34].

1.3. Two-electron spectroscopy versus EELS

The two-electron coincidence spectroscopy referred to as (e,2e) spectroscopy is a well-established technique for measurement of binding energies and momentum densities in atoms and molecules [59]. It can also be utilized to study the electronic structure of solids [60–62]. In the (e,2e) reaction an incident electron knocks out a target electron. The scattered and ejected electrons are subsequently detected in coincidence. There are at present two different modes of the (e,2e) reaction on solids: in transmission geometry with high-energy incident electrons [60] and in reflection geometry with medium- [62] and low-energy [63] incident electrons. It turns out that the low-energy (e,2e) spectroscopy in reflection geometry is very suitable for studying surface phenomena, in particular, secondary emission mechanism from solid surfaces.

The energy distribution of electrons scattered from a solid surface can be divided conventionally in two parts: true secondary emission features and energy losses. They are usually considered and discussed separately. In contrast, the recently developed (e,2e) spectroscopy on surfaces [61–63] allows in some cases to uncover the relation between the features in the spectra which are due to energy losses and true secondary emission structures. In the (e,2e) spectrum a pair of time-correlated electrons resulting from the interaction of a single incident electron with the surface is detected, the momenta of both electrons are measured.

Let us consider the scenario that one of the detected electrons may be the inelastically scattered primary electron, which lost part of its energy for exciting a plasmon, and the second ejected electron is the result of a plasmon decay. If this scattering mechanism is dominant then, in the two-dimensional energy distribution of correlated electron pairs (referred to as (e,2e) spectrum), a maximum will be observed at electron energies $E_1 = E_e$ and $E_2 = E_p - \hbar\omega_p$, where E_e is energy of ejected electron, whose energy does not depend on the primary energy (E_p).

As described in the introduction, the main features observed, that are in the inelastic X-ray scattering, in the electron energy loss spectra and in optical absorption spectra, are usually interpreted in terms of exciton and plasmon excitations [34,51,52,64]. The physical picture is that an electron excited from the valence band and positive hole left in the valence band form a bound "exciton" state. On the other hand in an insulator, the collective plasma oscillations can occur only through the excitation of electron–hole pairs, which is a mechanism similar to that forming the excitons. It should be noted however that the dispersion properties of these two modes are quite different, as discussed below.

The following expression was suggested by Egri [65] for the plasma frequency in nonmetals:

$$(\hbar\omega_x)^2 = (\hbar\omega_f)^2 + (E_x)^2, \quad (2)$$

where $\hbar\omega_x$ is the plasmon energy, ω_f is the free electron plasma frequency of the valence electrons, and E_x is the lowest transverse exciton energy. This conclusion derives from considerations of the microscopic dielectric function of an excitonic system [66], which is modeled by two discrete lines situated at E_x and E_g, respectively. Here E_g is the energy gap. The total oscillator strength is fixed by the f-sum rule, and the relative strengths depend on the properties of the system under consideration. The two extreme cases of insulators and semiconductors are considered. In an insulator, where the localized Frenkel exciton is the appropriate model, the oscillator strength is concentrated on E_x, whereas in semiconductors, where the Wannier model is applicable, the dominant transition is at E_g, where E_g is the band gap. On the basis of this consideration we could suggest the existence in the dielectric of the plasmon mode associated with the electron excitation from the valence band to the exciton state.

2. Experimental details

We applied (e,2e) spectroscopy in reflection mode (Fig. 1) [63] in combination with EELS and total (target) current spectroscopy (TCS) [67] for studying the mechanism of SEE from LiF films excited by 22–50 eV incident electrons.

Experiments were carried out in UHV conditions with a base pressure in the 10^{-10} Torr range. The residual magnetic field within the vacuum chamber was reduced to less than 5 mG using Helmholtz coils. A silicon wafer with the (0 0 1)

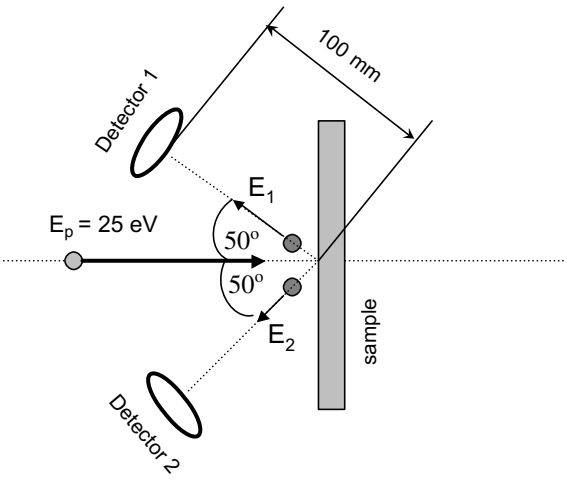

Fig. 1. Geometrical arrangement of the experiment.

plane parallel to the surface was mounted on a movable holder and was cleaned in the vacuum by resistive heating. It was used as a substrate for LiF film deposition. A Faraday cup (FC) was placed on the axis of the electron gun behind the sample and was used for incident current measurement when the sample is moved off-axis.

Before placing into the vacuum the silicon wafer was cleaned in NH_4OH–H_2O_2–H_2O (1:1:5) solution, rinsed in distilled water and etched in HF acid. In vacuum it was outgassed and heated to 1200 °C until low energy electron diffraction patterns from Si(1 0 0) surface appeared. LiF deposition on the Si(1 0 0) surface was performed from a Mo crucible heated by electron bombardment. The effective thickness of the film was estimated by measuring the change of surface potential during film evaporation and comparing these data with data in references [40,68]. The structure and morphology of the films were controlled by scanning electron microscopy and high-resolution transmission electron microscopy.

The geometry of the two-electron coincidence experiment is shown in Fig. 1. A time-of-flight (TOF) technique was used for measuring the energies of both correlated electrons. The TOF energy analysis is based on the measurement of the transit time T of an electron that traverses a distance L in a field-free space between the sample and detector. The kinetic energy of a slow electron, when relativistic effects are negligible, is

$$E = (m/2)(L/T)^2,$$

where m is the rest electron mass. A reference point on the time scale is obtained by pulsing the incident electron beam. An electron gun produces a pulsed electron beam with a pulse width of less than 1 ns and repetition rate of 4×10^6 Hz.

Position-sensitive detectors with resistive anodes were used for electron detection. Each of the two detectors consists of two micro-channel plates in a Chevron arrangement with a resistive anode (Quantar Technology, Model 3394). A grounded grid (Copper mesh, 92% transmission) is mounted in front of the first MCP, allowing the application of a 200 V accelerating voltage between the grid and MCP for increased detection efficiency. A fast pulse timing signal is taken from an additional 30 mm diameter Ti plate (0.4 mm thickness) mounted behind the resistive anode. An additional insulating polyimide film was placed between the plate and the resistive anode to minimize the risk of electrical breakdown.

When an incident electron generates a correlated pair of electrons and the detectors detect them, two pulses from Constant Fraction amplifiers start two time-to-amplitude converters (TAC). A stop pulse to both TAC comes from a logic unit that delivers a stop pulse only when two delayed and shaped pulses from the detectors and a delayed trigger pulse from the generator coincide within a time window of 200 ns. The coincidence time window of 200 ns was chosen to ensure that for a given flight distance of 100 mm we can detect all the electrons in the range from E_p (20–50 eV) down to 0.5–0.6 eV. This coincidence window allows a repetition rate of electron pulses as high as 5×10^6 Hz. In our experiment the time separation between incident electron pulses was set to 250 ns, which is 50 ns larger than the low limit of 200 ns (coincidence time window) to decrease the probability of an accidental coincidence from the slow "tail" electron generated by a previous incident pulse with an electron generated by the next pulse within the preset 200 ns coincidence window. The accidental coincidences in the measured spectrum originate mostly from the events when two, or more, electrons, within the same pulse of the incident beam, impinge onto the surface simultaneously and two electrons generated by two different primary electrons are detected within the coincidence window. In order to decrease the accidental coincidence rate, it is desirable to have less than one electron per pulse. This requirement limits the average incident electron current. In the present experiment the average incident current was in the 10^{-13}–10^{-14} A range, and that implies less than one electron per incident pulse in average.

Besides the timing pulses, the electron arrival positions on the detectors were measured. The position sensitivity of the detectors allowed the measurement "in parallel" of angular distribution of electrons, the observation of electron diffraction patterns, the estimation of the electron beam size and the measurement of the position-dependent flight time that takes into account the difference in

flight distances for electrons arriving, for example, at the center or at the edge of the detector. The arrival positions of electrons on the detectors were computed by position encoders that amplify and

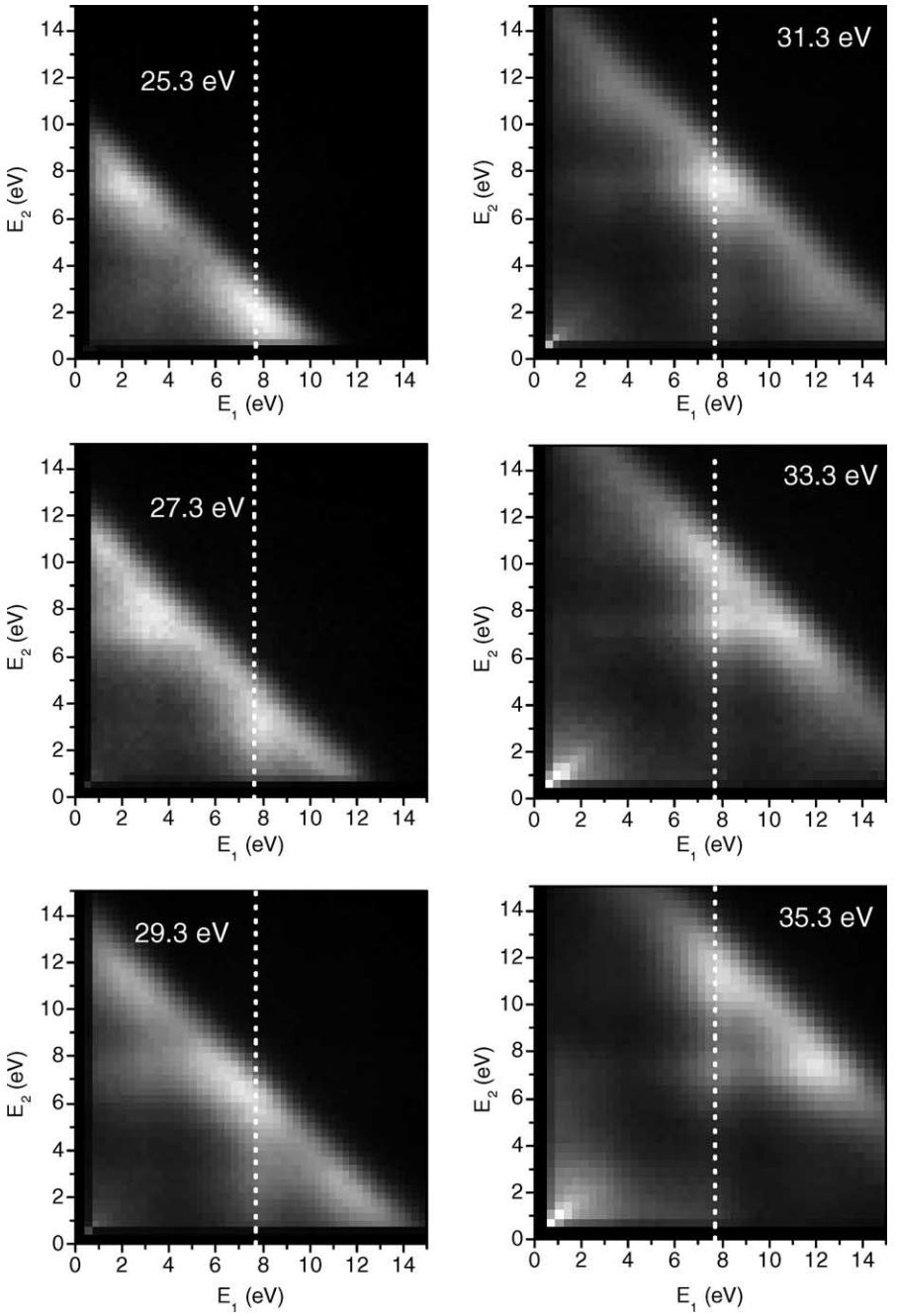

Fig. 2. Set of 2D energy distributions of correlated electron pairs excited by incident electrons from "thick" LiF film. Numbers indicate the incident energy. Dashed white lines mark maxima in the distributions with the same projections on E_1 axis.

process simultaneous pulses from each of the four corners of the resistive anode of each detector. The SCA pulses from the TAC1 and TAC2 gate the output pulses from the position encoders. Three analogue pulses from one detector and three pulses from the other representing the electrons' arrival times T_1, T_2 and positions on the detectors (x_1, y_1, x_2, y_2), are processed by the ADCs and stored in a list-mode file in a computer. In this way the measured distribution of correlated electron pairs presents a six-dimensional array, which then can be projected on any two-dimensional distribution such as E_1 vs E_2. An MPA-3 multi-parameter acquisition system (FAST ComTec) was used for data collection.

The above-described two-electron coincidence spectrometer can be used for measuring low energy electron energy loss spectra by switching off the coincidence conditions in the electronic setup. The characteristics of such spectrometer are described in [58].

3. Energy distribution of correlated electron pairs from a LiF film excited by low-energy primary electrons

The energy spectra of secondary electrons excited from a LiF film by an electron beam with various primary energies possess two main features at about 7 and 11 eV [58]. The energy positions of these maxima do not depend on the incident energy, which indicates that these two features are mainly determined by the target properties rather then by the scattering dynamics of the external projectile.

In a (e,2e) experiment one measures the two-dimensional energy distribution of time-correlated electron pairs resulting from the scattering of a single incident electron from the LiF film. A set of two-dimensional energy distributions of correlated electron pairs, or in other words (e,2e) spectra are shown in Fig. 2. The numbers on the spectra denote the primary electron energy. Each spectrum is symmetric with respect to the diagonal between the E_1 and E_2 axes because of the symmetry of the experiment with respect to the diagonal of the two electron detectors. The white dashed lines indicate maxima that have the same projection on the E_1 axes in all presented spectra. It means that one electron of the pair in the maximum is preferentially emitted with the same energy of about 7.5 eV independently of the incident electron energy. To underline this finding we show in Fig. 3 the projections onto the E_1 axis of the two-dimensional energy distributions, which are taken at various primary energies in the range 22.3–42.3 eV. It is

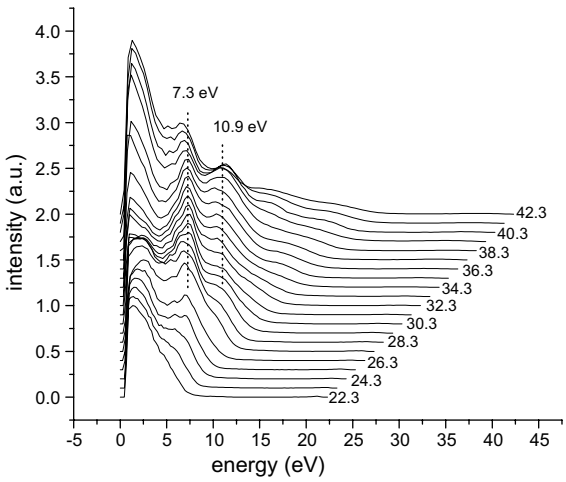

Fig. 3. Projections of the two-dimensional energy distributions on the E_1 axis. Numbers at curves indicate the incident energy.

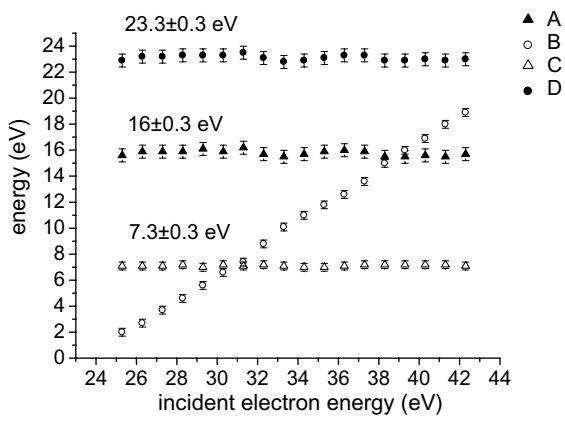

Fig. 4. Energy positions of scattered (B) and ejected (C) electrons, as well as incident electron energy loss (D) and binding energy of valence electron (A) for the scattering reaction in the maxima of 2D distributions (marked in Fig. 2 by white lines) presented as a function of the incident electron energy.

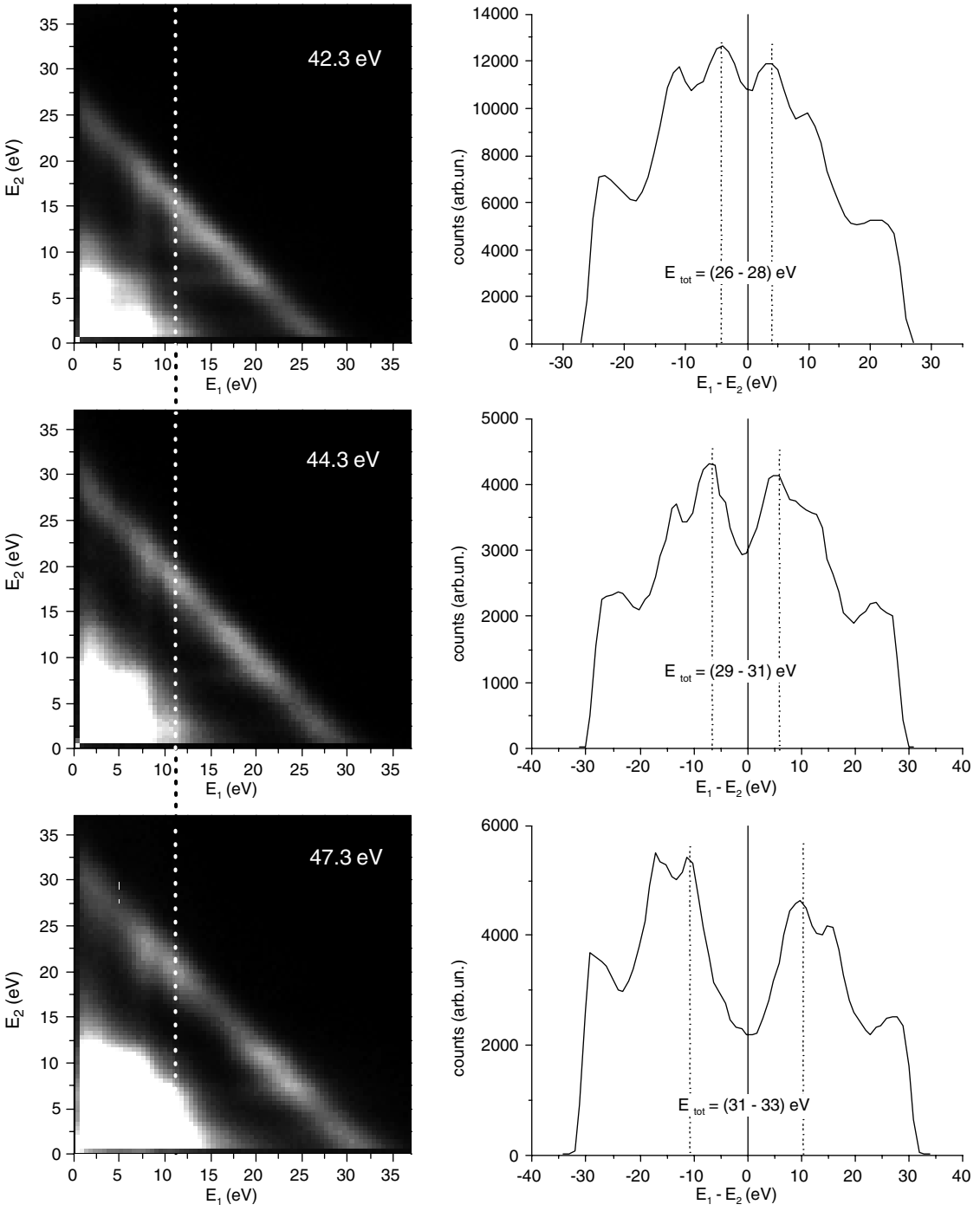

Fig. 5. 2D energy distributions of correlated electron pairs from LiF film measured at various primary energies (left column) and energy sharing distributions along the ridges of the corresponding 2D spectra (right column). The white dashed line in the left column marks the maxima with one electron of the pair having energy of 10.9 eV. Dashed lines in the right column show corresponding maxima in the sharing distributions.

seen that at primary energy of about 25 eV the maximum at 7.3 ± 0.3 eV start to appear.

It becomes more prominent at higher primary energies and moves toward lower energy for $E_p > 38$ eV. The second maximum at 10.9 ± 0.3 eV appears at about 30 eV of primary energy. We focus now on the maximum in the 2D spectrum, where one electron has energy 7.3 ± 0.3 eV. The energies of both correlated electrons from this maximum are presented in Fig. 4 as a function of the incident electron energy in curves B and C. The binding energy of the excited valence electron (A), as well as the energy lost by the incident electron (D), are presented also. These results show that the energy loss of 23 ± 0.3 eV causes the ejection of the electron with energy (7.3 ± 0.3) eV from the valence band at binding energy of (16 ± 0.3) eV. Now let us consider the maximum in the (e,2e) spectra where one of the electrons has an energy of 10.9 eV. We analyze the (e,2e) spectra taken for various primary energies, as indicated in Fig. 5, in the same way as was done for the 7.3 eV maximum. Fig. 6 shows the result of such analysis. The ejected electron (B) has always energy of 10.9 ± 0.3 eV, the energy lost by the primary electron (C) is 26.8 ± 0.4 eV and the binding energy (D) of the valence electron is 15.8 ± 0.3 eV.

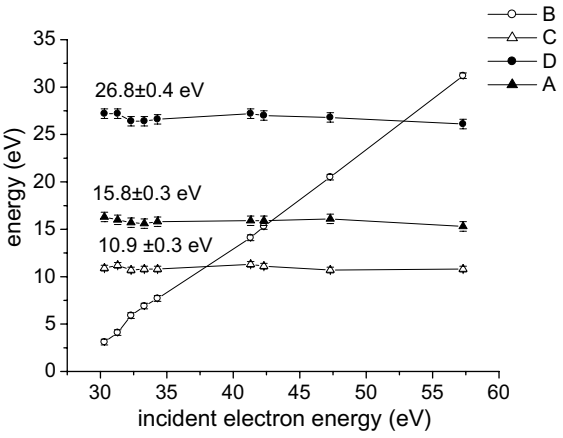

Fig. 6. Energy positions of scattered (B) and ejected (C) electrons, as well as incident electron energy loss (D) and binding energy of valence electron (A) for the scattering reaction in the maxima of 2D distributions (marked in Fig. 5 by white line) presented as a function of the incident electron energy.

4. Discussion

4.1. The origin of secondary emission features of LiF film

The above presented (e,2e) experimental results can be summarized as follows:

(1) Electron energy loss of 23 ± 0.3 eV is "responsible" for the electron ejection with the energy of 7.3 ± 0.3 eV. In other words the ejection of the electron with energy of 7.3 ± 0.3 eV occurs due to the decay of the collective excitation with energy of 23.3 ± 0.3 eV.
(2) Electron energy loss of 26.8 ± 0.4 eV causes the 10.9 ± 0.3 eV electron ejection or, equivalently, the emission of the electron with 10.9 ± 0.3 eV energy is due to the decay of the collective excitation with energy of 26.8 ± 0.4 eV.

The nature of energy losses at 23 and 26.8 eV is questionable. Fields et al. [35] measured electron energy loss spectra on LiF(1 0 0) and LiF(1 1 0) as a function of momentum transfer. On both surfaces they observed energy losses at 23 and 26 eV for large momentum transfer (>1 Å^{-1}). When momentum transfer decreases two energy losses merge to 25 eV maximum, which corresponds to the plasmon excitation in LiF. In our experiment

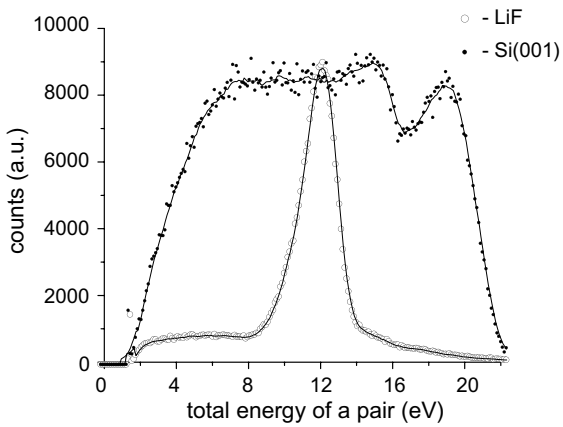

Fig. 7. Total energy distributions for clean Si(0 0 1) surface (full circles) and thin LiF film (open circles). It is seen that in the case of "thin" LiF film deposited on the Si(0 0 1) surface the contribution from LiF is dominant in the (e,2e) spectrum.

with low energy primary electrons we can expect a large momentum transfer for energy losses of 23 and 26.8 eV. Indeed, if we assume for the initial and final states of the incident electron the free electron-like parabolic dispersion, the energy loss of 24 eV by 30 eV primary electrons would correspond to the momentum transfer of 1.5 Å^{-1}, e.g. in the vicinity of the LiF Brillouin zone boundary. In [69] it was considered the influence of the periodic potential on the plasmon energy in metals and semiconductors. Due to plasmon Bragg diffraction the splitting of the plasmon energy near the Brillouin zone boundary into two ''nearly-free-plasmon'' bands was predicted. The plasmon energy splitting for a semiconductor (Ge) was predicted as large as 2 eV [69]. It means we could expect a similar splitting of plasmon energy in LiF for large momentum transfer.

If the observed energy losses at 23 and 26.8 eV correspond to the plasmons excitations, the emission features at 7.3 and 10.9 eV are due to their decay via electron ejection.

Alternative explanation of the energy losses and, by consequence, emission maxima in the secondary emission spectrum of LiF film could be the following. The excitonic states at about 10.6 and 12.5 eV are populated upon the impact of the projectile electron. Subsequently the excitonic states auto-ionize via exciton–exciton interaction. The energy with respect to the vacuum level of the

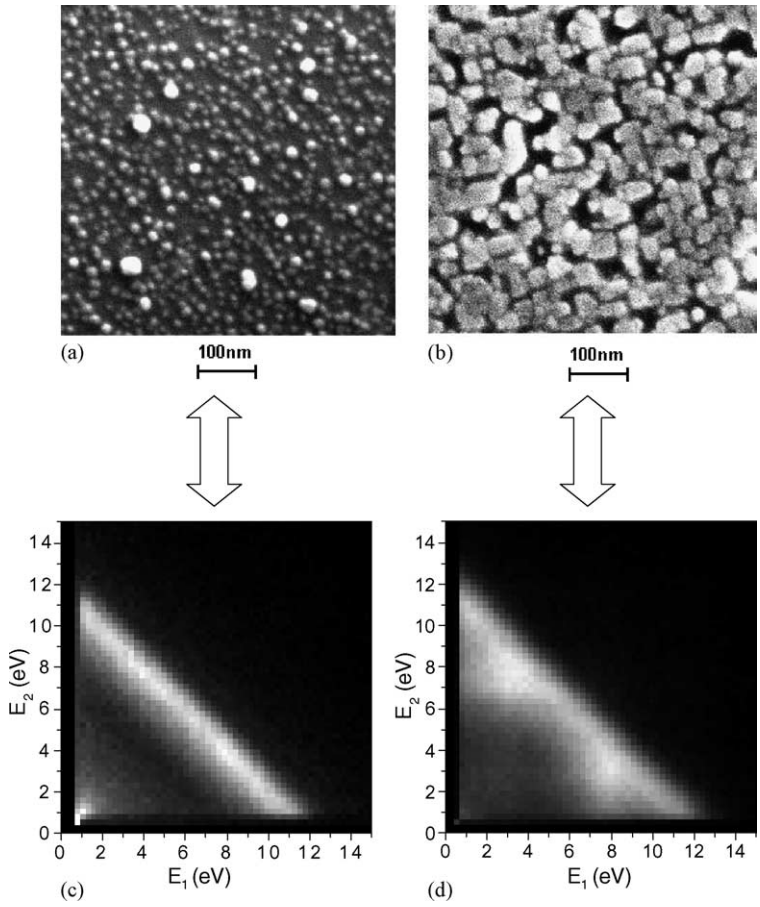

Fig. 8. SEM images of ''thin'' (a) and ''thick'' (b) LiF films on Si recorded at 3 kV, with an in-lens secondary electron detector, at working distance of 1 mm. Comparison of 2D energy distributions for these ''thin'' (c) and ''thick'' (d) LiF films measured at the same primary energy.

resulting electrons will then be localized around $(E_{ex} - (E_g - E_{ex}) - \chi)$ which gives approximately 7 and 11 eV as the localized position of this peaks in the secondary electron energy spectrum.

4.2. Thickness dependence of the secondary emission mechanism of LiF film

To check whether the observed features in the (e,2e) spectra depend on the film thickness we measured spectra for various LiF film thickness. For a thin film the plasmon-related features in the (e,2e) spectra are not observed although the contribution from LiF is dominant in the spectrum. Fig. 7 shows total energy distributions of correlated electron pairs excited from clean Si(0 0 1) and from thin LiF film deposited on Si(0 0 1). A corresponding two-dimensional energy distribution is shown in Fig. 8c. For comparison, a similar energy distribution for a thick LiF layer is presented in Fig. 8d. To define the terms "thin" and "thick" in our context we present images of the films taken with a LEO 1555 Field Emission Scanning Electron Microscope (FESEM) in Fig. 8a and b. The cross-sectional image of the "thick" film allows an estimate of the thickness of the film of about 100–150 Å. The surface morphology of the LiF film clearly displays an island structure. The "thick" film consists of islands with the size of 50–100 Å. As revealed in Fig. 8(b), the substrate (Si) surface is not completely covered. This was confirmed by TCS (diode method). In contrast, the "thin" film looks more homogeneous and the substrate surface is almost completely covered (Fig. 8a). The effective thickness of this film is estimated to be about 30–50 Å. This analysis suggests that the plasmon- and exciton-assisted (e,2e) reaction requires a certain thickness (island size) of LiF film and does not occur in a thin film.

5. Conclusion

The presented experimental results demonstrate a unique capability of the two-electron coincidence spectroscopy for studying scattering mechanism of low energy electrons from insulator. The two-dimensional energy distributions of correlated electron pairs visualize the exciton/plasmon-assisted SEE mechanism of a LiF film. The combination of (e,2e) spectroscopy and EELS allows the determination of the energy band parameters of the LiF film and a consistent energy balance analysis of the low energy electron scattering from the surface. It has been shown that the mechanism of secondary emission from LiF film depends on the film thickness and its structure.

Acknowledgements

The authors thank A. Morozov and L. Pravica for their help in the software design, T. Sergeant for assistance, S. Key and G. Light in the mechanical workshop in the Physics Department at UWA for technical support.

References

[1] J.W. Taylor, P.L. Hartman, Phys. Rev. 113 (1959) 1421.
[2] S.W. Duckett, P.H. Metzger, Phys. Rev. A 137 (1965) 953.
[3] M. Roessler, W.C. Walker, J. Phys. Chem. Solids 28 (1967) 1407.
[4] R.T. Poole, J.G. Jenkin, J. Liesegang, R.C.G. Leckey, Phys. Rev. B 11 (1975) 5179.
[5] R.T. Poole, J. Liesegang, R.C.G. Leckey, J.G. Jenkin, Phys. Rev. B 11 (1975) 5190.
[6] M. Piacentini, Solid State Commun. 17 (1975) 697.
[7] G. Roy, G. Singh, T.E. Gallon, Surf. Sci. 152/153 (1985) 1042.
[8] P.A. Cox, A.A. Williams, Surf. Sci. 175 (1986) 1782.
[9] T.E. Gallon, Surf. Sci. 206 (1988) 365.
[10] P. Wurz, J. Sarnthein, W. Husinsky, G. Betz, P. Nordlander, Y. Wang, Phys. Rev. B 43 (1991) 6729.
[11] D. Ewing, F. Seitz, Phys. Rev. 50 (1936) 760.
[12] T.B. Grimley, Proc. Phys. Soc. London 71 (1958) 749.
[13] A.B. Kunz, T. Miyakawa, S. Oyama, Phys. Status Solidi 34 (1969) 581.
[14] L.J. Page, E.H. Hygh, Phys. Rev. B 1 (1970) 3472.
[15] R.C. Chaney, E.E. Lafon, C.C. Lin, Phys. Rev. B 4 (1971) 2734.
[16] G.S. Painter, Int. J. Quantum Chem., Quantum Biol. Symp. 5 (1971) 501.
[17] D.M. Drost, J.L. Fry, Phys. Rev. B 5 (1972) 684.
[18] M.R. Hayns, J. Phys. C 5 (1972) 15.
[19] F. Perrot, Phys. Status Solidi B 52 (1972) 163.
[20] N.E. Brener, Phys. Rev. B 7 (1973) 1721.
[21] D.J. Mickish, A.B. Kunz, J. Phys. C 6 (1973) 1723.
[22] G.E. Laramore, A.C. Switendick, Phys. Rev. B 7 (1973) 3615.
[23] A.B. Kunz, Phys. Rev. B 12 (1975) 5890.

[24] A. Zunger, A.J. Freeman, Phys. Rev. B 16 (1977) 2901.
[25] A.B. Kunz, Phys. Rev. B 26 (1982) 2056.
[26] A.B. Kunz, C.P. Flynn, J. Phys. C 16 (1983) 1659.
[27] V.A. Lobatch, B.E. Kulyabin, V.P. Zhukov, N.I. Medvedeva, Phys. Status Solidi B 158 (1990) 239.
[28] H. Tatewaki, E. Miyoshi, Surf. Sci. 327 (1995) 129.
[29] M. Rohlfing, S.G. Louie, Phys. Rev. Lett. 81 (1998) 2312.
[30] D.M. Roessler, W.C. Walker, J. Opt. Soc. Am. 57 (1967) 835.
[31] E.L. Shirley, L.J. Terminello, J.E. Klepeis, F.J. Himpsel, Phys. Rev. B 53 (1996) 10296.
[32] F.J. Himpsel, L.J. Terminello, D.A. Lapiano-Smith, E.A. Eklund, J.J. Barton, Phys. Rev. Lett. 68 (1992) 3611.
[33] R.T. Poole, J.G. Jenkin, J. Liesegang, R.C.G. Leckey, Phys. Rev. B 11 (1975) 5179.
[34] W.A. Caliebe, J.A. Soininen, E.L. Shirley, C.-C. Kao, K. Hämäläinen, Phys. Rev. Lett. 84 (2000) 3907.
[35] J.R. Fields, P.C. Gibbons, S.E. Schnatterly, Phys. Rev. Lett. 38 (1977) 430.
[36] J.J.M. Michiels, L. Hedin, J.E. Inglesfield, Phys. Rev. B 50 (1995) 11386.
[37] H. Tatewaki, Phys. Rev. B 60 (1999) 3777.
[38] A. Akkerman, A. Breskin, R. Chechik, A. Gibrekhterman, in: R.A. Baragiola (Ed.), Ionization of Solids by Heavy Particles, Plenum Press, New York, 1993, p. 359.
[39] B. Henke, J. Liesegang, S.D. Smith, Phys. Rev. B 19 (1979) 3004.
[40] F. Golek, E. Bauer, Surf. Sci. 369 (1996) 415.
[41] A.I. Gusarov, S.V. Murashov, Surf. Sci. 320 (1994) 36.
[42] S. Kiyono, T. Muranaka, A. Okazaki, Technology Reports of the Tohoku University 42 (1) (1977) 247.
[43] D. Pines, Elementary Excitations in Solids, Benjamin, New York, 1966.
[44] R.A. Ferrell, Phys. Rev. 111 (1958) 1214.
[45] M.S. Chung, T.E. Everhart, Phys. Rev. B 15 (1977) 4699.
[46] N.B. Gornyi, L.M. Rakhovich, S.F. Skirko, Sov. Phys. J. 10 (1967) 15.
[47] C. Horie, Prog. Theor. Phys. 21 (1) (1959) 113.
[48] A.B. Kunz, T. Miyakawa, S. Oyama, Phys. Stat. Solidi 34 (1969) 581.
[49] T. Miyakawa, Solid State Communs. 25 (1978) 133.
[50] M. Creuzburg, Z. Phys. 196 (1966) 433.
[51] C. Gout, F. Pradal, J. Phys. Chem. Solids 29 (1968) 581.
[52] F. Golek, W.J. Sobolewski, Phys. Stat. Solidi 210 (1) (1998) R1.
[53] F. Golek, Phys. Stat. Solidi (b) 177 (1993) K5.
[54] F. Golek, W.J. Sobolewski, Phys. Stat. Sol. (b) 216 (1999) R1.
[55] D.A. Lapiano-Smith, E.A. Eklund, F.J. Himpsel, Appl. Phys. Lett. 59 (1991) 2174.
[56] F.J. Himpsel, in: H.-J. Freund, E. Umbach (Eds.), Adsorption on Ordered Surfaces of Ionic Solids and Thin Films, Springer Series in Surface Science, vol. 33, Springer-Verlag, Berlin, 1993.
[57] Kenji Kimura, Gou Andou, Kaoru Nakajima, Nuclear Instruments & Methods in Physics Research, Section B-Beam Interactions with Materials and Atoms 164 (2000) 933.
[58] S.N. Samarin, O.M. Artamonov, D.K. Waterhouse, J. Kirschner, A. Morozov, J.F. Williams, Rev. Sci. Instr. 74 (2003) 1274.
[59] Erich Weigold, I.E. McCarthy, Electron Momentum Spectroscopy, Kluwer Academic/Plenum Publishers, New York, 1999.
[60] M. Vos, I.E. McCarthy, Rev. Mod. Phys. 67 (1995) 713.
[61] J. Kirschner, O.M. Artamonov, A.N. Terekhov, Phys. Rev. Lett. 69 (1992) 1711.
[62] S. Iacobucci, L. Marassi, R. Camilloni, S. Nannarone, G. Stefani, Phys. Rev. B 51 (1995) 10252.
[63] O.M. Artamonov, S. Samarin, J. Kirschner, Appl. Phys. A (Mater. Sci. Process.) A65 (6) (1997) 535.
[64] G. Roy, G. Singh, T.E. Gallon, Surf. Sci. 152/153 (1985) 1042.
[65] I. Egri, Solid State Commun. 44 (1982) 563.
[66] I. Egri, J. Phys. C: Solid State Phys. 12 (1979) 5471.
[67] S.A. Komolov, Total Current Spectroscopy of Surface, Gordon and Breach, Philadelphia, PA, 1992.
[68] R. Schlaf, B.A. Parkinson, P.A. Lee, K.W. Nebesny, G. Jabbour, B. Kippelen, N. Peyghambarian, N.R. Armstrong, J. Appl. Phys. 84 (1998) 6729.
[69] R. Girlanda, M. Parrinello, E. Tossatti, Phys. Rev. Lett. 36 (1976) 1386.